Infrastructure and Environment Scotland 2nd Postgraduate Conference
2nd September 2014
The University of Edinburgh, Edinburgh

Partition of unity finite element method for time-dependent diffusion problems: an error estimate for the method

Muhammad Iqbal[1,*], Heiko Gimperlein[2], M. Shadi Mohamed[1], Omar Laghrouche[1]
[1]Institute for Infrastructure and Environment, Heriot-Watt University
[2]Maxwell Institute for Mathematical Sciences and Department of Mathematics, Heriot-Watt University
[*](Email: mi130@hw.ac.uk)

ABSTRACT

This paper investigates an error estimate for the partition of unity method solution of time dependent diffusion problem. An enriched finite element method is used to solve the problem and the results are compared to a predefined error estimate. Gaussian functions with two different variations are used to compute the results and the one with better approximation is then used for the subsequent analysis. The problem is analyzed with different values of time steps i.e. 0.001, 0.01 and 0.1. The L^2 error for the solution and derivatives of the solution is computed and compared to the defined error estimate. It is confirmed that at each time step the actual error is bounded by the error estimate.

1. INTRODUCTION

The partition of unity finite element method (PUFEM) [1] is a powerful technique used to numerically solve complex engineering problems governed by steady-state and time-dependent partial differential equations. The method has shown remarkable reduction in computation time and memory requirements for complex engineering problems involving time-dependent partial differential equations. Melenk and Babuška [1] developed the mathematical background of the partition of unity method. They showed how the partition of unity finite element method can be used to employ the structure of the differential equation under consideration to construct effective and robust methods.

The PUFEM incorporates special functions into the finite element method (FEM) to solve the problem. These special functions called enrichment functions are chosen based on an approximate analytical solution of the problem. To a great extent the effectiveness of the PUFEM depends on the proper selection of enrichment functions. A wisely chosen enrichment function can provide better approximation than standard polynomial shape functions used in the classical finite element method. Strouboulis *et al*. [2] showed that the choice of enrichment function affects the solution of the problem. They used harmonic basis functions to obtain better accuracy corresponding to the problem of the elliptical void in an infinite medium.

The PUFEM is effectively used to solve engineering problems both in solid and fluid mechanics. In solid mechanics it has shown its effectiveness in problems involving discontinuities, voids, cracks and complex geometries. In fluid dynamic applications it is beneficial to represent strong continuous variations in the solution using relatively coarse meshes, for example, in viscous regions associated with wall bounded flows. Munts *et al*. [5] investigated the effectiveness of PUFEM for convection-diffusion problems. O'Hara *et al.* [3] used it for transient analysis of sharp thermal gradients. They used global-local enrichment functions to problems of transient heat transfer involving localized features. Laghrouche and Mohamed [4] used it for solving the Helmholtz equation in two dimensions. They constructed oscillatory shape functions as the product of polynomial shape functions and either Bessel functions or planer waves. In their work they dealt with the diffraction of an incident plane wave by a rigid circular cylinder. Duarte and Kim [6] used PUFEM for accurately modeling a crack using enrichment functions from the asymptotic expansion of the elasticity in the neighborhood of the crack. Mohamed *et al*. [7] used PUFEM for the solution of time dependent diffusion problems. They used multiple enrichment function to obtain the results. In their work they compared the results of both finite element method and PUFEM and concluded that in general the PUFEM shows higher accuracy than the conventional FEM for a fixed number of degrees of freedom. They showed that PUFEM requires less computational resources for the time-dependent diffusion problems than the standard FEM. A full description of previous work can be found in [7].

In our present work we use PUFEM to solve the time-dependent diffusion problem and then compare the results to pre-defined error estimates.

We use two different variations of exponential enrichment functions to solve the problem. For both the enrichment functions we compute the L^2 norm error for the solution and its derivatives and then select the enrichment function with better approximation for all further analyses.

2. THEORY

2.1 Problem formulation

Given an open domain $\Omega \subset \mathbb{R}^2$ with boundary Γ and given time interval]0,T], we are interested to solve the following transient diffusion equation

$$\frac{\partial u}{\partial x} - \lambda \Delta u = f(t, \boldsymbol{x}), \quad (t, \boldsymbol{x}) \in]0, T] \: x \: \Omega \tag{1}$$

Where $\boldsymbol{x} = (x, y)^T$ are the spatial coordinates, u is the temperature, t is the time variable, λ is the diffusion coefficient and $f(t, \boldsymbol{x})$ represents the effect of internal sources/sinks. We consider an initial condition

$$u(t = 0, \boldsymbol{x}) = u_0(\boldsymbol{x}), \quad (\boldsymbol{x} \in \Omega) \tag{2}$$

where $u_0(\boldsymbol{x})$ is a prescribed initial field. The aforementioned equations are subjected to a Robin type boundary condition

$$\frac{\partial u}{\partial \boldsymbol{n}} + hu = g(t, \boldsymbol{x}), \quad (t, \boldsymbol{x}) \in]0, T] \: x \: \Gamma \tag{3}$$

where $\boldsymbol{n}$ is the outward normal on the boundary Γ and g is a given boundary function.

To solve equation (1)-(3) numerically, we divide the time interval into N_t subintervals $[t_n, t_{n+1}]$ with duration $\Delta t = t_{n+1} - t_n$ for $n = 0, 1, 2, \dots N_t$. We discretize equation (1) in time using an implicit scheme.

$$\frac{u^{n+1} - u^n}{\delta t} - \lambda \Delta u^{n+1} = f(t_{n+1}, \boldsymbol{x}) \tag{4}$$

or

$$-\Delta u^{n+1} + k u^{n+1} = F \tag{5}$$

where

$$F = k(\delta f(t_{n+1}, \boldsymbol{x}) + u^n), \quad k = \frac{1}{\lambda \delta t}$$

To solve equation (5) with the finite element method we first multiply the equation with a weighting function, W, and then integrate over Ω

$$-\int_\Omega W \, \Delta u^{n+1} d\Omega + \int_\Omega W \, k u^{n+1} d\Omega = \int_\Omega W \, F d\Omega \tag{6}$$

Now suppose we have a function, S , such that

$$S = W \nabla u^{n+1} = \begin{pmatrix} W \dfrac{\partial u^{n+1}}{\partial x} \\ W \dfrac{\partial u^{n+1}}{\partial y} \end{pmatrix} \tag{7}$$

Taking divergence of the function S and applying the divergence theorem, we get

$$\int_\Omega (\nabla W . \nabla u^{n+1} + \mathrm{W} k u^{n+1}) d\Omega - \int_\Gamma W \nabla u^{n+1} . n \, d\Gamma = \int_\Omega WF \, d\Omega \tag{8}$$

Substituting the boundary conditions and rearranging, we get

$$\int_\Omega (\nabla W . \nabla u^{n+1} + W k u^{n+1}) d\Omega + \int_\Gamma W(k u^{n+1} - g) \, d\Gamma = \int_\Omega WF \, d\Omega \tag{9}$$

Equation (9) is the weak form of the problem to be solved with PUFEM.

3. PARTION OF UNITY MEHTOD TO SOLVE THE PROBLEM

To solve the weak form (9) with FEM, the temperature u over each element is approximated using the nodal values and polynomial shape functions

$$\mathrm{u} = \sum_{\mathrm{i}=1}^{\mathrm{n}} \mathrm{N_i u_i} \tag{10}$$

In PUFEM the nodal values, $\mathrm{u_i}$, are written as a combination of enrichment functions. In our case we considered the following sum of global exponential functions to enrich the solution space

$$F_{enr} = G_1, G_2, G_3, \dots \dots G_Q \tag{11}$$

We considered two types of global exponential functions. 1st enrichment function is termed as G_{q_1} and the 2nd is termed as G_{q_2}.

$$G_{q_1} = \frac{e^{-\left(\frac{R_0}{C}\right)^q} - e^{-\left(\frac{R_c}{C}\right)^q}}{1 - e^{-\left(\frac{R_c}{C}\right)^q}} \tag{12}$$

$$G_{q_2} = \frac{e^{-\left(\frac{R_0^2}{C^2}\right)^q} - e^{-\left(\frac{R_c^2}{C^2}\right)^q}}{1 - e^{-\left(\frac{R_c^2}{C^2}\right)^q}} \tag{13}$$

$q = 1, 2, 3, \ldots . Q$

with $R_0 \coloneqq |\,\boldsymbol{x} - \boldsymbol{x_c}|$ being the distance from the function control point $\boldsymbol{x_c}$ to the point $\boldsymbol{x}$. The constants $R_c = \sqrt{\frac{14}{1.195}}$ and $C = \sqrt{\frac{1}{1.195}}$ control the shape of the exponential function, G_q. Alturi and Zhu [8] also used an enrichment function similar to (12) with $q = 2$ as a weight function in the context of meshless methods for solving the linear Poisson equation. Similar functions are used when $q = 1$ in [5, 9] and $q = 2$ in [3, 10]. We use both the enrichment functions G_{q_1} and G_{q_2} to find the L^2 norm error for solution and derivatives of the solution. In the subsequent theory, the derivatives are given only for G_{q_1}. Similar derivatives can also be found for G_{q_2}.

Considering the aforementioned enrichment functions, the nodal values are written as

$$u_i = \sum_{q=1}^{Q} A_j^q\, G_q \tag{14}$$

where the FEM is now used to find the unknowns A_j^q instead of the nodal values. Using (14) to re-write (10), we get

$$u = \sum_{j=1}^{M} \sum_{q=1}^{Q} N_j A_j^q\, G_q \tag{15}$$

The product of the enrichment function with the polynomial shape function is considered as new shape function $P_{(j-1)q+Q}$, i.e.

$$P_{(j-1)q+Q} = N_j G_q \tag{16}$$

The derivatives of the new shape function are given as

$$\frac{\partial P_{(j-1)q+Q}}{\partial x} = G_q \frac{\partial N_j}{\partial x} - N_j (x - x_c) \frac{q}{C^q} \frac{e^{-\left(\frac{R_0}{C}\right)^q}}{1 - e^{-\left(\frac{R_c}{C}\right)^q}} R_0^{(q-2)}$$

and

$$\frac{\partial P_{(j-1)q+Q}}{\partial y} = G_q \frac{\partial N_j}{\partial y} - N_j (y - y_c) \frac{q}{C^q} \frac{e^{-(\frac{R_0}{C})^q}}{1 - e^{-(\frac{R_c}{C})^q}} R_0^{(q-2)}$$

The second derivatives of the new shape function are given as

$$\frac{\partial^2 P_{(j-1)q+Q}}{\partial x^2} = [-2 \frac{\partial N_j}{\partial x} (x - x_c) \frac{q}{C^q} \frac{e^{-\left(\frac{R_0}{C}\right)^q}}{1 - e^{-\left(\frac{R_c}{C}\right)^q}} R_0^{(q-2)}$$
$$+ N_j \frac{q}{C^q} \frac{e^{-\left(\frac{R_0}{C}\right)^q}}{1 - e^{-\left(\frac{R_c}{C}\right)^q}} (1 - \frac{q}{C^q} R_0^{(q-2)} (x - x_c)^2$$
$$+ \frac{q-2}{R_0^2} (x - x_c)^2]$$

and

$$\frac{\partial^2 P_{(j-1)q+Q}}{\partial y^2} = [-2 \frac{\partial N_j}{\partial y} (y - y_c) \frac{q}{C^q} \frac{e^{-\left(\frac{R_0}{C}\right)^q}}{1 - e^{-\left(\frac{R_c}{C}\right)^q}} R_0^{(q-2)}$$
$$+ N_j \frac{q}{C^q} \frac{e^{-\left(\frac{R_0}{C}\right)^q}}{1 - e^{-\left(\frac{R_c}{C}\right)^q}} (1 - \frac{q}{C^q} R_0^{(q-2)} (y - y_c)^2$$
$$+ \frac{q-2}{R_0^2} (y - y_c)^2]$$

3.1 Definition of error estimate

In this section we define the error estimate for the method. We will then compare the results obtained by the PUFEM to the error estimate.

Let us define

$$u(\boldsymbol{x}, t) = \frac{t - t_n}{t_{n+1} - t_n} u^{n+1}(\boldsymbol{x}) + \frac{t_{n+1} - t}{t_{n+1} - t_n} u^n(\boldsymbol{x})$$

and

$$\hat{u}(\boldsymbol{x}, t) = u(\boldsymbol{x}, t_{n+1}), \hat{f}(\boldsymbol{x}, t) = f(\boldsymbol{x}, t_{n+1}), t \in [t_n, t_{n+1}]$$

Let u and U be the numerical and exact solution respectively of the equation (1), with

$$U(0, \boldsymbol{x}) = U_0(\boldsymbol{x}) \text{ and } U|_{\Omega} = 0$$

then

$$\int_{\Omega} |U(t_{(n+1)}, \boldsymbol{x}) - u(t_{(n+1)}, \boldsymbol{x})|^2 dx + \iint_{t_n}^{t_{n+1}} |\nabla(U - u)|^2 d\boldsymbol{x} dt \le \eta_2^2 + \eta_4^2 \tag{17}$$

where

$$\eta_2^2 = \int_{t_n}^{t_{n+1}} ||f - \partial_t u - \Delta u||^2_{H^{-1}(\Omega)}$$
$$\le \int_{t_n}^{t_{n+1}} dt \int_{\Delta} (f - \partial_t u - \Delta u)^2\, d\Omega$$
$$\cong \int_{\Delta} (f^{n+1} - \frac{u^{n+1} - u^n}{\delta t} - (\frac{\partial^2 u^{n+1}}{\partial x^2} + \frac{\partial^2 u^{n+1}}{\partial y^2}))^2 \frac{\delta t}{2} d\Omega$$

$$+\int_{\Delta}(f^n-\frac{u^{n+1}-u^n}{\delta t}-(\frac{\partial^2 u^n}{\partial x^2}+\frac{\partial^2 u^n}{\partial y^2}))^2\frac{\delta t}{2}d\Omega \quad (18)$$

and

$$\eta_4^2=\int_{t_n}^{t_{n+1}}||\nabla(u-\hat{u}||^2_{L^2(\Omega)}$$

$$=\int_{t_n}^{t_{n+1}}\left(\frac{t_{n+1}-t}{t_{n+1}-t_n}\right)^2 dt\int_{\Delta}[(\frac{\partial u^{n+1}}{\partial x}-\frac{\partial u^n}{\partial x})^2$$

$$+(\frac{\partial u^{n+1}}{\partial y}-\frac{\partial u^n}{\partial y})^2$$

$$=\frac{1}{(t_{n+1}-t_n)^2}(t^2_{n+1}-t_{n+1}(t^2_{n+1}-t^2_n)$$

$$+\frac{1}{3}(t^3_{n+1}-t^3_n)\int_{\Delta}[(\frac{\partial u^{n+1}}{\partial x}-\frac{\partial u^n}{\partial x})^2+(\frac{\partial u^{n+1}}{\partial y}-\frac{\partial u^n}{\partial y})^2]d\Omega \quad (19)$$

We will calculate the quantities defined in (17), and will then compare it with the summation of two error terms η_2^2 and η_4^2.

4. NUMERICAL ANALYSIS

Numerical results of the PUFEM for the proposed problem are presented here. We consider a square domain $\Omega=[0,2]\times[0,2]$. We solve the transient equations (1) - (3) with reaction term $f(t,\boldsymbol{x})$, the boundary function g and the initial condition $u_0(\boldsymbol{x})$ being explicitly calculated such that the exact solution is given by

$$U=x^{20}y^{20}(2-x)^{20}(2-y)^{20}(1-e^{-\lambda t}) \quad (20)$$

To quantify the error for both the enrichment functions, we compute the relative L^2-norm error for the solution and derivatives of the solution, defined by

$$L^2=\frac{||u-U||_{L^2(\Omega)}}{||U||_{L^2(\Omega)}} \quad (21)$$

$$L_x^2=\frac{||u_x-U_x||_{L^2(\Omega)}}{||U_x||_{L^2(\Omega)}} \quad (22)$$

$$L_y^2=\frac{||u_y-U_y||_{L^2(\Omega)}}{||U_y||_{L^2(\Omega)}} \quad (23)$$

where u, u_x and u_y are the numerical solution and its derivatives with respect to x and y respectively. Similarly U, U_x and U_y are the exact solution and its derivatives with respect to x and y respectively.

4.1 Comparison of different enrichment functions

We solve the problem using two different variations of Gaussian enrichment functions G_{q_1} and G_{q_2}. For all the analyses the parameter $\lambda=0.1$. The initial analysis is carried out using both type of enrichment functions using a 7x7 mesh, $Q=6$ and $\Delta t=0.001$. The solution is obtained for 50 time steps. A comparison of results using G_{q_1} and G_{q_2} is presented in Table 1. The results are presented at different time steps, i.e. at time step 1, 20, 40 and 50. The L^2 error for the solution and its derivatives is computed.

Table 1 compares the results of L^2-norm error for G_{q_1} and G_{q_2}. In the table $\boldsymbol{L^2}$ represents the relative error for the solution while $\boldsymbol{L_x^2}$ and $\boldsymbol{L_y^2}$ are the relative error in derivatives of the solution w.r.t x and y respectively. From results of $\boldsymbol{L^2}$ error for G_{q_1} and G_{q_2}we notice that the values are slightly higher for G_{q_1}than G_{q_2}. At 1st time step it is 0.647% for G_{q_1}while 0.633% for G_{q_2}. But values of $\boldsymbol{L_x^2}$ and $\boldsymbol{L_y^2}$ are less for G_{q_1} than G_{q_2}. The same trend is observed at all the time steps. Both the error estimates η_2^2 and η_4^2 as well as the quantities defined in equation (17) involve derivatives of the analytical and exact solution, so we are more interested in better values for $\boldsymbol{L_x^2}$ and $\boldsymbol{L_y^2}$. As G_{q_1}yields better values for both $\boldsymbol{L_x^2}$ and $\boldsymbol{L_y^2}$ than G_{q_2}, we select G_{q_1} for all our subsequent analysis with $Q=2,3\dots6$. All the further analyses are carried out with three different values of time steps, i.e. $\Delta t=0.001, 0.01$ and 0.1.

Table 1. Comparison of relative error for G_{q_1} and G_{q_2} enrichment functions

	Relative error for G_{q_1}			**Relative error for G_{q_2}**		
Time step No.	L^2 **%**	L_x^2 **%**	L_y^2 **%**	L^2 **%**	L_x^2 **%**	L_y^2 **%**
1	0.647	3.499	3.502	0.633	3.819	3.818
20	0.699	3.476	3.479	0.670	3.801	3.801
40	0.715	3.474	3.478	0.679	3.800	3.801
50	0.720	3.474	3.478	0.682	3.800	3.800

4.2 Calculation of error estimate for the method

We compute the quantities defined by equation (17). These quantities calculate the error in the numerical solution compared to the exact solution and error in the derivatives of numerical solution in comparison to the derivatives of exact solution. As defined by equation (17), the summation of these two quantities should be less than or equal to the summation of two error terms η_2^2 and η_4^2. These two error terms are defined by equations (18) and (19) respectively. Figures 1(a)-1(c) show the comparison of these quantities. In graphs the term ''Error'' represents the actual error in the method as defined by equation (17), and the term ''EB'' represents the summation of error terms η_2^2 and η_4^2. Solution is obtained using different number of enrichment functions $Q=2,3,\dots6$, In Figures 1(a)-

1(c) results are shown at 50th time step for three different values of Δt, i.e. $\Delta t = 0.001, 0.01$ and 0.1. Results of the figures 1(a)-1(c) show that the actual error in the method is well below the defined estimates. The difference between these actual errors and the defined estimates increases with the increasing number of enrichment functions. This suggests that if we increase the number of enrichment functions we get much better results. The values of error estimates η_2^2 and η_4^2 also depend on the selectin of the value of time step Δt. Figure 2 represent the results of relative error at t=0.5 for different values of time steps Δt.

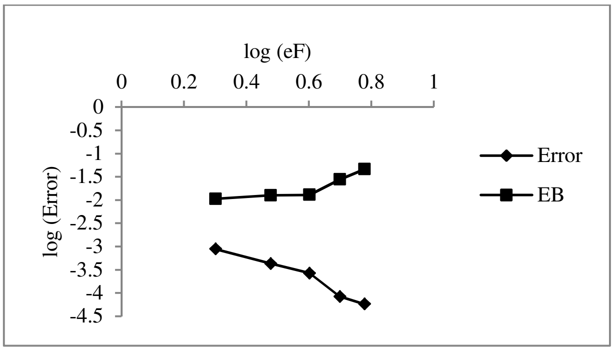

Figure 1(a). Comparison of actual error and error estimate at 50th time step for Δt = 0.001(t=0.05)

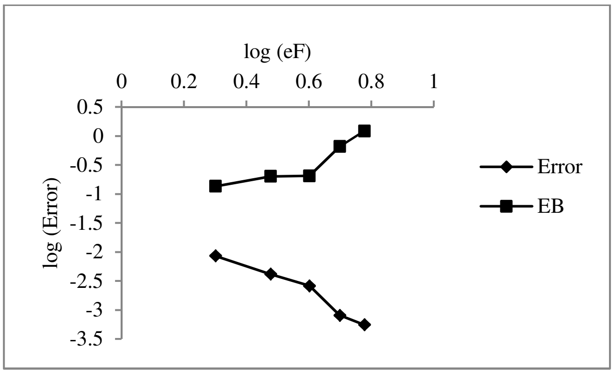

Figure 1(b). Comparison of actual error and error estimate at 50th time step for Δt = 0.01(t=0.5)

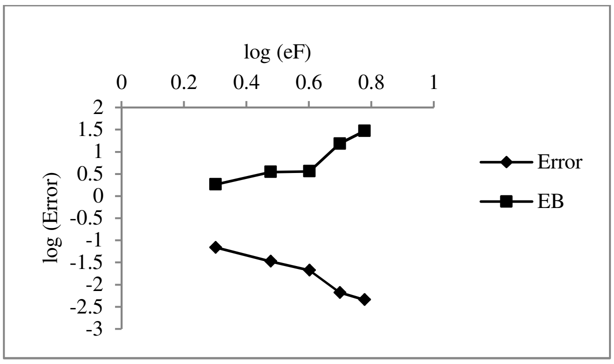

Figure 1(c). Comparison of actual error and error estimate at 50th time step for Δt = 0.1(t=5)

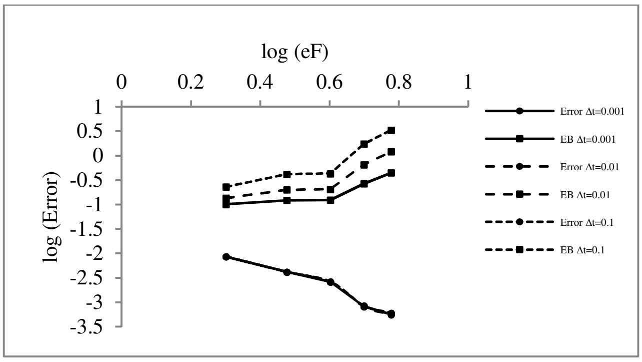

Figure 2. Comparison of actual error and error estimate at t=0.5 and Δt = 0.001, 0.01 and 0.1

Figure 2, shows the effect of selecting different values of time step Δt. By changing the value of time step value Δt, the actual error stays almost at the same position. As shown in the graph these values almost overlap each other for all the three values of time steps Δt, however the value of predefined estimate is strongly dependent on the selection of value of Δt. Figure 2 depicts that with increasing the value of Δt, the values of the error estimates also increase. For higher values of Δt, the difference between the actual error and the defined error estimate increases. Equations (18) and (19) show the dependency of these error estimates on the value of Δt.

4.3 Conditioning of the partition of unity method

In this section we show some of the results for the conditioning of the PUFEM. Figures 3(a)-3(c) show the conditioning for partition of unity method at 50th time step for $\Delta t = 0.001, 0.01$ and 0.1. From figures 3(a)-3(c) it is clear that the conditioning number increases very sharply as the number of enrichment functions increases. This is anticipated because the enrichment functions start with relatively sharp gradients closer to the source and then rapidly flatten out at higher orders. A similar behaviour is also reported in [7]. Mohamed *et al.* showed that using higher number of enrichment functions, the same error can be achieved using a lower number of degrees of freedom. However conditioning affects the accuracy of the PUFEM.

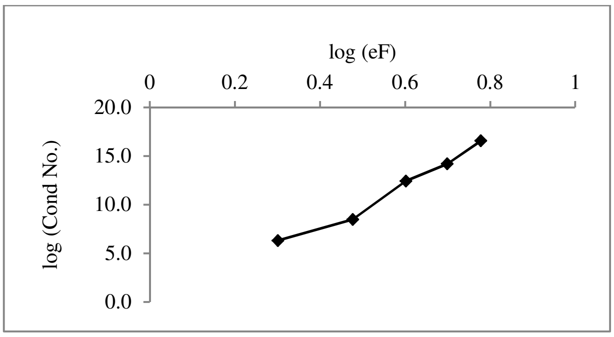

Figure 3(a). Conditioning of the method with increasing number of enrichment functions for Δt = 0.001(t=0.05)

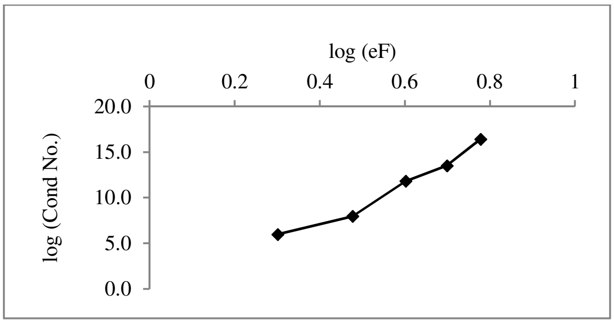

Figure 3(b). Conditioning of the method with increasing number of enrichment functions for Δt = 0.01(t=0.5)

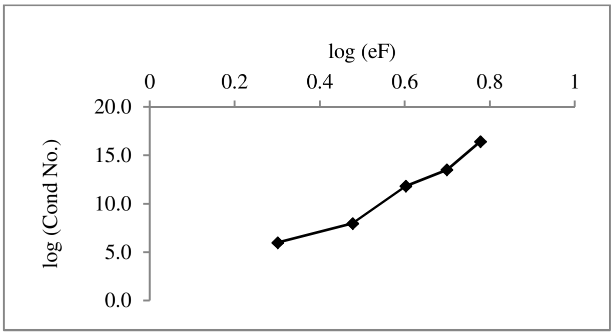

Figure 3(c). Conditioning of the method with increasing number of enrichment functions for Δt = 0.1(t=5)

Figures 3(a)-3(c) show that with the increasing number of enrichment functions, the conditioning degrades very quickly. The same kind of behaviour is observed with all the values of time step Δt. This puts a limit on the use of higher enrichment functions. For our analyses we use up to 6 enrichment functions.

5. CONCLUSIONS

In this paper, we used the PUFEM to solve the time dependent diffusion equation. We calculated the errors in the solution and its derivatives for the PUFEM. We defined an error estimate and compared the actual error in the method with the defined error estimate. We used two different enrichment functions and showed its effect on the solution. We also show the effect of increasing enrichment function on the conditioning number of the resulting system of equations. Based on the analyses, we can draw the following conclusions:

- Results of the actual error are well below the defined error estimate.
- Results are obtained with three different values of time step Δt, and for each value of Δt, the results are within the range of error estimate, which show the effectiveness of the method for time dependent diffusion problem.
- The definition of the error estimates is dependent on the selection of time step value Δt, higher value of time step means higher value of the error estimate.
- Selection of enrichment function affects the accuracy of the solution. By choosing an enrichment function intelligently, one can obtain better results.
- Increasing the number of enrichment functions produce better results but the enrichment functions can be increase only up to certain limit after which the system becomes ill-conditioned.

6. REFERENCES

[1] Melenk, J. M. & Babuška, I. (1996). The partition of unity finite element method: basic theory and applications. *Computer methods in applied mechanics and engineering*, *139*(1): 289-314.

[2] Strouboulis, T., Copps, K. & Babuska, I. (2000). The generalized finite element method: an example of its implementation and illustration of its performance. *International Journal for Numerical Methods in Engineering*, *47*(8): 1401-1417.

[3] O'Hara, P., Duarte, C. A. & Eason, T. (2011). Transient analysis of sharp thermal gradients using coarse finite element meshes. *Computer Methods in Applied Mechanics and Engineering*, *200*(5): 812-829.

[4] Laghrouche, O. & Mohamed, M. S. (2010). Locally enriched finite elements for the Helmholtz equation in two dimensions. *Computers & structures*, *88*(23): 1469-1473.

[5] Munts, E. A., Hulshoff, S. J. & Des Borst, R. (2003). The partition-of-unity method for linear diffusion and convection problems: accuracy, stabilization and multiscale interpretation. *International journal for numerical methods in fluids*, *43*(2): 199-213.

[6] Duarte, C. A. & Kim, D. J. (2008). Analysis and applications of a generalized finite element method with global–local enrichment functions. Computer Methods in Applied Mechanics and Engineering, 197(6): 487-504.

[7] Shadi Mohamed, M., Seaid, M., Trevelyan, J. & Laghrouche, O. (2013). A partition of unity FEM for time dependent diffusion problems using multiple enrichment functions. International Journal for Numerical Methods in Engineering, 93(3): 245-265.

[8] Atluri, S. N. & Zhu, T. (1998). A new meshless local Petrov-Galerkin (MLPG) approach in computational mechanics. Computational mechanics, 22(2): 117-127.

[9] Van der Meer, F. P., Al-Khoury, R. & Sluys, L. J. (2009). Time-dependent shape functions for modeling highly transient geothermal systems. International journal for numerical methods in engineering, 77(2): 240-260.

[10] O'Hara, P., Duarte, C. A. & Eason, T. (2009). Generalized finite element analysis of three-dimensional heat transfer problems exhibiting sharp thermal gradients. Computer Methods in Applied Mechanics and Engineering, 198(21): 1857-1871.